Marine Geology xxx (2009) xxx–xxx

Contents lists available at ScienceDirect

Marine Geology

journal homepage: www.elsevier.com/locate/margeo

Mapping reef features from multibeam sonar data using multiscale morphometric analysis

S. Zieger [a,*], T. Stieglitz [b,c], S. Kininmonth [b]

[a] Institute for Cartography, Dresden University of Technology, Dresden, 01062, Germany
[b] AIMS@JCU, Australian Institute of Marine Sciences, Townsville, Queensland 4810, Australia
[c] School of Engineering and Physical Sciences, James Cook University, Townsville, Queensland 4811, Australia

ARTICLE INFO

Article history:
Received 26 August 2008
Received in revised form 28 April 2009
Accepted 1 June 2009
Available online xxxx

Communicated by D.J.W. Piper

Keywords:
geomorphology
submerged platform reef
multiscale analysis
morphometric analysis
Great Barrier Reef

ABSTRACT

Classification of seafloor habitats from geomorphological proxies is increasingly being applied to understand the distribution of benthic biota, particularly as more and larger datasets, collected with high-resolution multibeam echo sounders, are becoming available. With increased capacity to collect and use sonar data, there is a need for automated approaches to identify seafloor structures and habitats. For a survey area of approximately 2.5×2.5 km, a generic feature extraction algorithm similar to terrestrial topographic analysis has been developed and applied to a spatially complex submerged mid-shelf reef in the Great Barrier Reef lagoon. Multibeam data collected with a RESON Seabat 8101 was gridded at 1 m resolution, and an automated feature extraction method was applied that analyses the seafloor geomorphology to predict reef features from geomorphological proxies. Quadric surface fitting was used to determine various surface parameters based on multiple spatial scales. Subsequently, 6 morphometric feature types (plane, channel, ridge, pass, pit, and peak) were derived for all mapping scales. Weighted multiscale fuzziness was then applied to extract the dominant morphometric feature classes. Finally, seafloor morphology patterns in combination with seafloor rugosity measurements were analysed in order to predict reef features. These reef features cover significant patches of bioturbation beyond the submerged platform reef, as well as the dominant reef features such as outer-reef crest and inner-reef flat. Layback-corrected and manually classified towed video transects support the classification algorithms used to extract the reef features.

1. Introduction

Coral reefs are the largest biologically constructed features on Earth's seafloor. They are characterised by a great species diversity associated with high structural and ecological complexity. Much research has been devoted to understanding this complexity, particularly in the Great Barrier Reef (GBR). Hopley et al. (2007) provide a comprehensive overview of reefal geomorphology and its effect on distribution of biota on continental shelf scales. Describing the extensive variety in morphology (e.g. reef facies), biotic cover (corals, algae etc.), and substrate type is critical to understanding the coral reef environment (Hopley et al., 2007). However, inconsistency in scale for habitat identification has led to a variety of interpretations (González et al., 2006). Generally, the most commonly applied scale of habitat description is between reef types and not within one reef complex. With increasing availability of high-resolution multibeam sonar, the seafloor morphology can be mapped quickly on the scale of individual single reefs, but methods of translation to biological information are limited. In previous applications, habitats were classified manually by drawing polygons around similar regions in a derived shaded relief image, similar to the manual data analysis of satellite imagery (Buja, 2006).

Early geomorphology studies, e.g. by Orme et al. (1978); Davies et al. (1981); Johnson et al. (1982); Davies et al. (1983); Orme and Salama (1988), etc., were carried out on outer-shelf reefs using chiefly visual observations and aerial photography. Approximately 2500 reefs in the Great Barrier Reef have been mapped using aerial photography (Jupp et al., 1985). Early coral reef classification schemes adopted a threefold separation into juvenile, mature and senile reefs (Hopley, 1982). The deeper inter-reefal areas still lag behind in sophisticated research activities (Hopley et al., 2007), with the important exception of the GBR Seabed Biodiversity program (Pitcher et al., 2007), which used benthic dredge, bottom trawling, and visual census to document mid-shelf flat seafloor habitats.

Research in terrestrial landform classification has been conducted for decades, but seafloor mapping has lagged behind. A reason for this is the lack until recently of sufficiently high-resolution remote sensing techniques available for water covered landforms. Recently geospatial statistics have been applied in seafloor mapping (Iampietro et al., 2005; Wilson et al., 2007; Lanier et al., 2007; Lucieer and Pederson, 2008). To identify features and structures on the seafloor, morphology and rugosity (roughness) are essential attributes (Lundblad et al.,

* Corresponding author.
E-mail addresses: stefan.zieger@gmx.net (S. Zieger), thomas.stieglitz@jcu.edu.au (T. Stieglitz), s.kininmonth@aims.gov.au (S. Kininmonth).

0025-3227/$ – see front matter.
doi:10.1016/j.margeo.2009.06.002

2006; Jordan et al., 2006). Multibeam sonar systems provide a 3D terrain model with 100% coverage, which allows a meaningful definition of a number of derivative surface attributes (e.g. slope, curvature, etc.). For example, the "Bathymetric Position Index" (BPI), introduced by Weiss (2001), is commonly used to identify habitats (Lundblad et al., 2006; Wilson et al., 2007; Lanier et al., 2007). Mitchell and Hughes Clarke (1994) distinguished between seafloor types by analysing echo strength, slope, and curvature from sonar data. For curvature measurements, a paraboloid was fitted to a subset of soundings to separate between relief types (i.e. ridges, troughs and ponds).

The objective of this study is to apply a multiscale feature extraction algorithm to multibeam bathymetry data in order to automatically extract major reef features, including "standard" reef geomorphologic units such as outer-reef crest inner-reef flat, etc. but also previously undescribed units such as features controlled by macroscopic, meter-scale bioturbation.

2. Methods

2.1. Data collection

The study site is an isolated submerged mid-shelf reef locally known as "The Pinnacle" located in the GBR lagoon at 19°01′ South and 147°33′ East (Fig. 1). The base of the reef is at approximately 42 m depth, and the reef rises to 11 m in depth within less than 200 m distance. The survey area is approximately 2.5 × 2.5 km in size with the submerged platform reef in the centre. A subset of this data was used in the analysis presented here.

Bathymetry was recorded with a pole-mounted multibeam echosounder RESON Seabat 8101 with an operating frequency of 240 kHz. Vessel track and heading were recorded with a Differential Global Positioning System (Differential GPS/DGPS) and gyrocompass. The motion of the vessel was recorded with a TSS DMS dynamic motion sensor mounted at the centre of gravity of the vessel. Dynamic offsets were calculated from a patch test at a nearby shoal. The Seabat 8101 multibeam echosounder has 101 beams with an athwartship angle of 1.5° for each beam. It records bathymetry in a swath of a total width of effectively 5 to 7 times the water depth in rough and calm conditions respectively. The survey was carried out during calm to moderately calm conditions. Due to survey time constraints, tracks on the seafloor surrounding the shoal were spaced apart such that close to a 100% coverage was achieved (calculated based on a swath width of between 5 and 7 times the water depth), resulting in occasional data gaps and residual motion artefacts from regions where only outer-beam data are available. The comparatively shallow shoal was mapped with a significantly smaller track separation, generally achieving >50% swath overlap, resulting in 100% coverage.

Data was processed with the software SWATHED of the Ocean Mapping Group of the University of New Brunswick, Canada, and IVS Fledermaus. Sonar ranges measured with the echosounder were converted to depth by integrating the range, GPS, heading and motion data whereby the acoustic data were corrected for refraction using sound velocity profiles recorded at the start and end of each survey, and tidal water level variation was corrected for using high-resolution tidal predictions from the Australian Hydrographic Office (AHO).

The processed *xyz* data was converted into a digital bathymetric model (DBM) with a spatial resolution of 1 m by weighted gridding, whereby outer-beam data with a larger acoustic footprint was given a smaller weight than high-resolution inner-beam data (Hughes Clarke and Godin, 1993; Cartwright and Hughes Clarke, 2002). A constant beam angle results in a larger acoustic footprint on the seafloor of outer beams. Collected sonar resolution ranged approximately from 0.3 m to 3 m.

Due to the non-ideal rack separation in the deeper sections of the survey regions, outer-beam data is used. Some of this data is affected by an incomplete correction of the roll motion of the vessel due to difference in motion of the sonar and the hull (pole flexing), resulting in periodic small-scale, approximately linear artefacts perpendicular to the vessel track. Such artefacts are most pronounced on the deep seafloor (non-reefal areas). If strict hydrographical survey rules applied, this imperfect data should to be removed in the raw data processing. This would inevitably result in larger data gaps in the survey.

Instead we include these data in the DBM and demonstrate how a feature recognition algorithm can be employed to address such artefacts. In practice, many surveys are affected by similar artefacts, and we consider it useful to have an alternative tool available to take these artefacts into account.

2.2. Morphometric feature extraction

In terrestrial landform analysis, morphometry is used to measure the shape of landform units and their spatial distribution (Fisher et al., 2004). A morphometric class is determined by the geographical scale, and therefore a combination of spatial detail (resolution) and spatial extent (size) is required to delineate the class (Evans, 1980; Richards, 1981; Wood, 1996; Fisher et al., 2004).

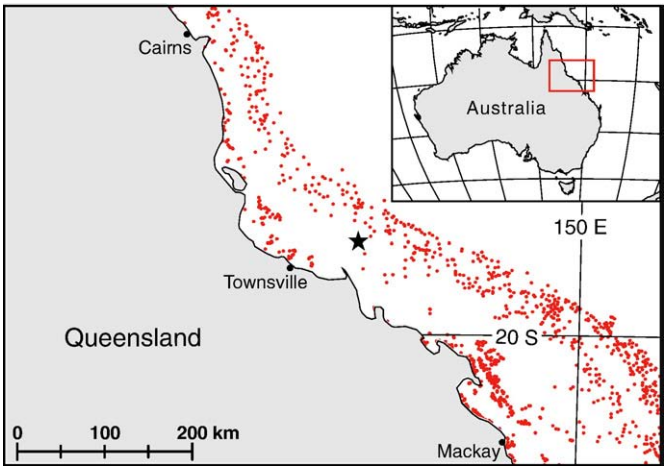

Fig. 1. Distribution of reefs within the Great Barrier Reef. The star indicates the study site, an isolated submerged reef shoal on the mid-shelf.

Please cite this article as: Zieger, S., et al., Mapping reef features from multibeam sonar data using multiscale morphometric analysis, Mar. Geol. (2009), doi:10.1016/j.margeo.2009.06.002

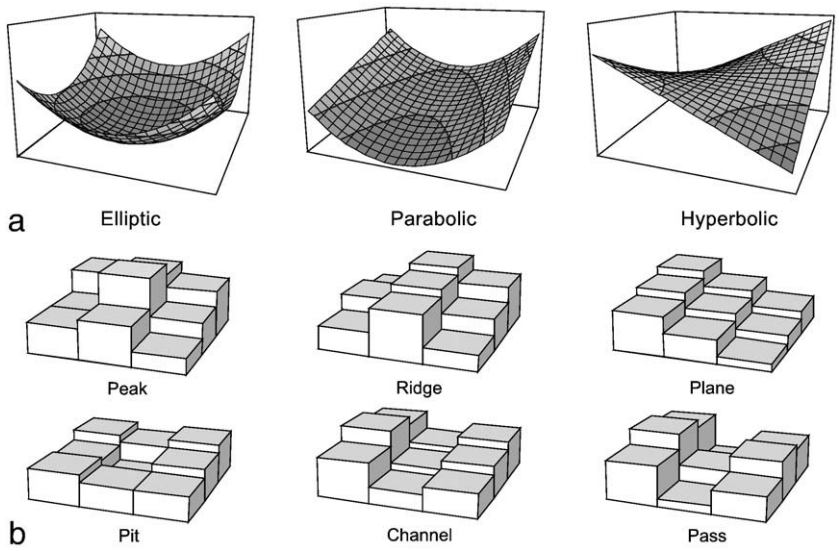

Fig. 2. Second-degree polynomials (a), are applicable to derive six morphometric feature classes (b), simplified by a 3×3 cell raster. Adapted from Wood (1996).

Therefore, terrain feature identification is generally based on a variety of resulting attributes, such as slope, aspect, curvature, rugosity, and surface type. Evans (1980) suggested that a bivariate quadratic function (second-degree polynomial) can be used to describe local surface areas numerically, here in the form of the matrix representation of conic sections for Cartesian coordinates (x,y):

$$f(x,y) = (1,x,y) \cdot \frac{1}{2}\begin{pmatrix} 2b_0 & b_1 & b_2 \\ b_1 & 2b_3 & b_4 \\ b_2 & b_4 & 2b_5 \end{pmatrix} \cdot \begin{pmatrix} 1 \\ x \\ y \end{pmatrix} \quad (1)$$

In principle, conic sections are related to morphometric feature types (Fig. 2a), where the correspondence is as follows: elliptic shapes refer to pits and peaks, parabolic forms to channels and ridges, and hyperbolic shapes to passes.

To examine the spatial extent, a dynamic filter kernel with least squares regression was applied to determine the 6 unknown surface coefficients (b_0..., b_5) by transforming Eq. (1) into a system of linear equations. The solution of such linear system is a common numeric problem that can be solved using matrix algebra.

Given the circular nature of morphological features in a reef, a circle was selected as the basic filter kernel with a spatial extent ranging from 5 to 35 m. To derive the 6 morphometric features (Fig. 2b), a set of 4 morphometric parameters was calculated. Following Evans (1980) and Wood (1996), the parameters slope (Eq. (2)), cross-sectional curvature (Eq. (3)), maximum (Eq. (4)) and minimum curvature (Eq. (5)) were used to identify the set of feature classes.

$$slope = \arctan\left(\sqrt{b_1^2 + b_2^2}\right) \quad (2)$$

$$crosc = -2 \cdot \frac{b_5 \cdot b_1^2 + b_3 \cdot b_2^2 - b_1 \cdot b_2 \cdot b_4}{b_1^2 + b_2^2} \quad (3)$$

$$cmax = -b_3 - b_5 + \sqrt{(b_3 - b_5)^2 + b_4^2} \quad (4)$$

$$cmin = -b_3 - b_5 - \sqrt{(b_3 - b_5)^2 + b_4^2} \quad (5)$$

Once morphometric parameters were processed, a decision tree that describes 6 morphometric feature classes was applied, as illustrated in Fig. 3. At this stage, 2 tolerance values, minimum slope (*slopemin*) and minimum cross-sectional curvature (*croscmin*), were introduced to suppress classification noise in the final outcome.

The surface parameterisation was implemented in Python (a fast, open-source, object-orientated programming language), and additional procedures were written for Environmental Systems Research Institute's (ESRI) Arc/Info workstation using Arc Macro Language (AML). Python scripts are platform-independent and ESRI embedded Python into ArcGIS software products, since the release of version 9 (Buttler, 2005). Note that this subsection of the computation requires most of the time for processing. For instance, a 5×5 filter kernel takes 433 elements per second to process (5.5 h), whereas for a 19×19 kernel speed already decelerates down to 33 elements per second (3 days in total) using an Intel 2.2 GHz processor. Three days sounds slow, but consider that more than 8 million grid cells have to be processed for each scale.

2.3. Multiscale fuzziness

The intermediate results are categorised into 6 morphometric features, processed with different kernel sizes. Importantly, the derived morphological structure at any one point is correlated with the geographical extent or spatial scale. For example, at a large-scale measurement a channel might be identified, while at smaller scales a ridge would be identified. Indeed, large-scale analysis will produce a near random-like distribution of all of the 6 morphometric features, whereas channels, ridges and planes will be produced primarily at small scales (Wood, 1996; Fisher et al., 2004).

To address this problem, fuzzy set theory has been used using fuzzy logic membership functions to solve ambiguity (or vagueness). Vagueness in geography has been used in several studies for fuzzy set analysis (Robinson, 1988; Fisher, 2000; Fisher et al., 2004). At various scales the Boolean membership may change and thus a location may be "composed of" different morphometric features at different spatial scales. In this case, the fuzzy membership μ_A in each of the 6 morphometric features, j, is given by a weighted average of

Please cite this article as: Zieger, S., et al., Mapping reef features from multibeam sonar data using multiscale morphometric analysis, Mar. Geol. (2009), doi:10.1016/j.margeo.2009.06.002

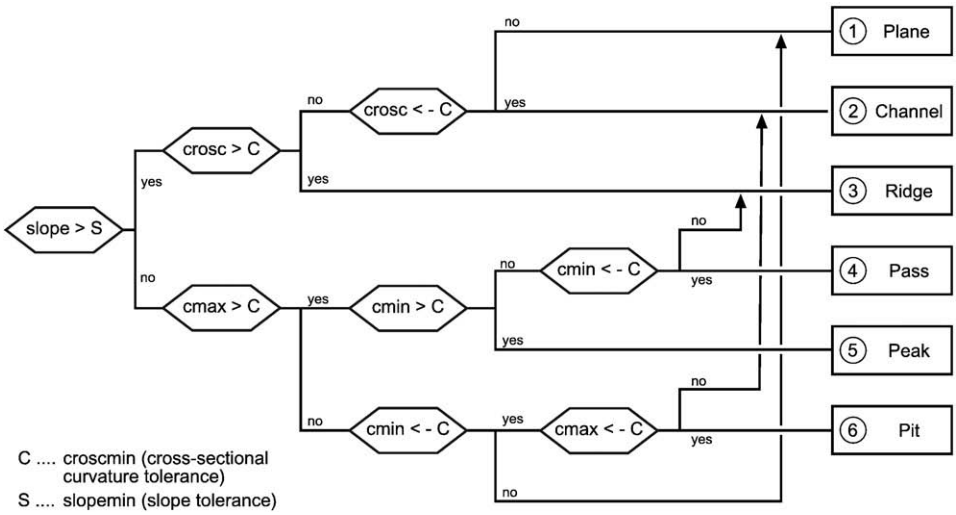

Fig. 3. Decision tree to derive six morphometric feature classes. Adapted from Wood (1996; Table 5.2).

the binary membership determined for each scale, i (Fisher et al., 2004, p. 110).

$$\mu_{Ax} = \frac{\sum_{i}^{n} \omega_i \cdot m_{Ax|si}}{\sum_{i}^{n} \omega_i} \tag{6}$$

In Eq. (6) ω is the weight corresponding to the scale i, where n represents the total number of scales. At this point, if vagueness exists at location x, a sufficient solution is to compute the dominant class by applying a modal operator to all fuzzy membership μ_{Ax} values. The variance of this fuzzy membership approach can be computed by the entropy, an evaluation of the arbitrariness of a system, whereas the normalised entropy E_x is given by Fisher et al. (2004):

$$E_x = -\frac{\sum_{j=1}^{6} \mu_{Ajx} \cdot \ln \mu_{Ajx}}{-\ln \frac{1}{6}} \tag{7}$$

2.4. Seafloor rugosity

Rugosity is one of the important attributes to describe seafloor features as a measure of roughness, but it is evidently not clearly defined in geospatial terms. Greene et al. (2004) define rugosity by variations of slope within a particular area of interest, whereas Dartnell (2000) uses the range of elevations inside the kernel window. A more sophisticated representation of surface roughness presented by Jenness (2002) calculates the ratio between surface and planar (projective) area. This ratio will be equal to 1 for flat planes and increases in value for more complex surfaces. The variance in planar direction is generally higher than in elevation; hence, the ratio is limited to an upper boundary value. Jenness (2002) ratio was embedded in Python and adapted to the size of the moving filter kernel (from originally 3×3 cells). The projective area can be summed up easily by counting raster cells, but to grid a surface, a triangulation algorithm is essential. Bourke (1989) provided an implementation of the Delaunay triangulation algorithm for American National Standards Institute (ANSI) C that was used in Python. The final rugosity dataset is a five-class raster image based on standard deviation class breaks (very low, low, moderate, high, extreme).

2.5. Reef feature mapping

Following Hopley (1982), the major division of morphological zones consists of the windward reef front, the outer-reef crest, the inner-reef flat, the lagoons and the leeward margins. The windward reef front and outer-reef crest are zones with a large variety of coral spices. Hopley (1982) showed that the outer-reef crest with windward reef front shows the highest growth rates of the reef. This high-energy zone is characterised by complex surface structures and significant coral formations interrupted by pockets and channels, referred to as spur-and-groove systems. The inner-reef flat is mostly radially shaped and less well defined. The coral density and growth rates are marginal in this zone. Mapped reef features (outer-reef crest, inner-reef flat), can be summarised by the main dependency of depth, morphology, and rugosity, which are the 3 compulsory datasets. Based on the data type of the morphometric feature dataset (integer numbers), mathematical morphology was applied as an image processing technique.

$$A \circ B = (A \ominus B) \oplus B \tag{8}$$

$$A \bullet B = (A \oplus B) \ominus B \tag{9}$$

Mathematical morphology can enhance or flatten structures using set operations e.g. to extract the skeleton or hull of an object. Morphological operations are generally composed of expanding (dilation) and shrinking (erosion) operations applied on binary images (raster cells either one or zero). The utilisation of these operations on an object A requires a structuring element B (i.e. filter kernel), whereas the structure element can adopt various shapes, but is commonly represented by a disc or rectangle. In Eq.(8) morphological opening is

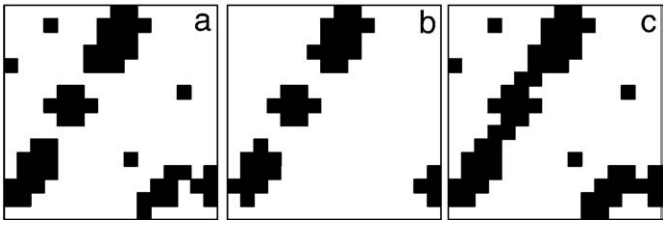

Fig. 4. Morphological opening (b) and closing (c) applied on the binary image (a) using a disk of 1 cell radius as structuring element.

Please cite this article as: Zieger, S., et al., Mapping reef features from multibeam sonar data using multiscale morphometric analysis, Mar. Geol. (2009), doi:10.1016/j.margeo.2009.06.002

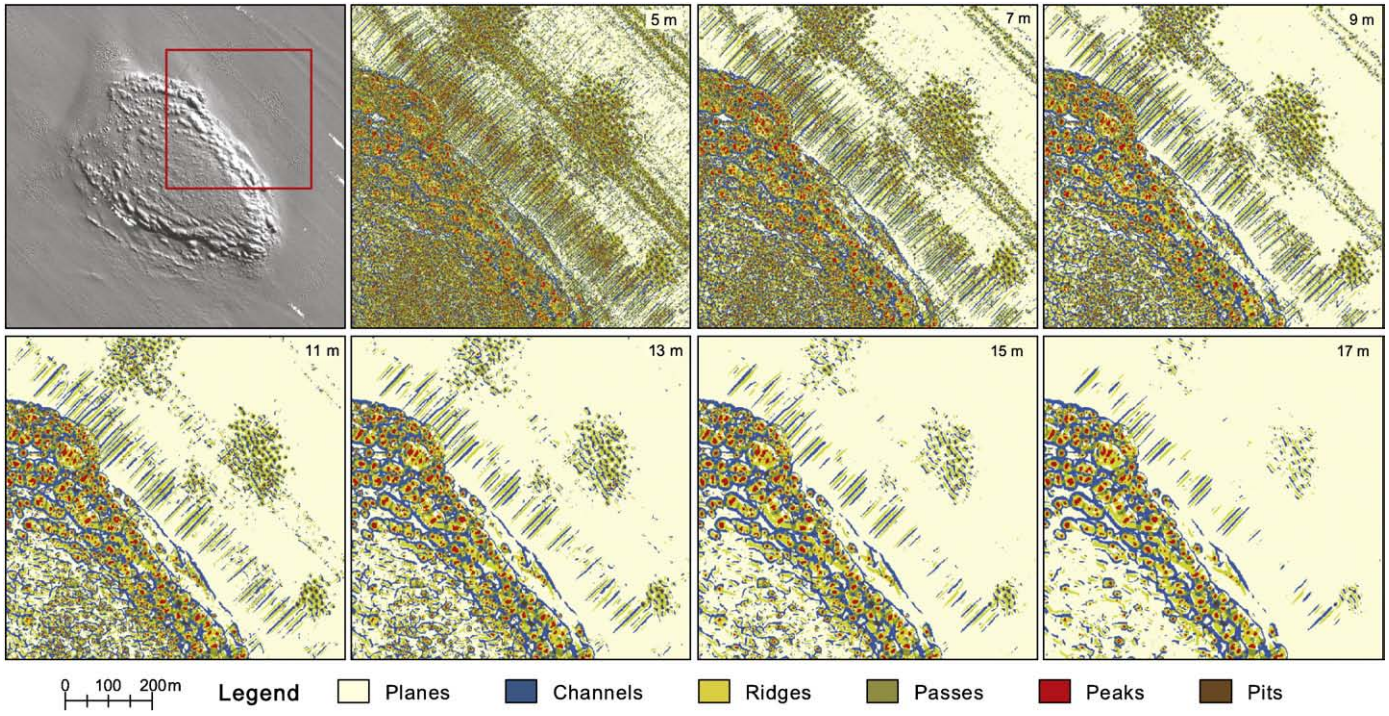

Fig. 5. Variation in spatial scale. The morphometric feature classifier is strongly affected by the spatial scale of measurement (subset of 5 to 17 m for the kernel size). Large-scale analysis produces a random-like distribution of all feature classes, whereas channel and ridges dominate at smaller scales (*slope* = 35°, *crosc* = 0.012).

defined by erosion ($A \ominus B$) followed by dilation ($A \ominus B$), which will remove all elements that are smaller than the structure element (smoothing filter). Closing (Eq. (9)) is the inverse operation of opening and is produced by the dilation followed by erosion, which is used to fill cracks or holes and to connect interrupted lines (Sierra, 1982). Opening operators are generally used to remove random noise from an image (Fig. 4b), whereas, closing operators (Fig. 4c) may be used to fix disconnected graphs in networks (i.e. contour lines). Reef feature mapping uses opening and closing operators and zonal statistics to produce joint areas of reef features based on distinctive morphometric features (i.e. peaks for coral boulders, or planes for reef flats).

Reef areas were automatically separated from non-reef areas (seafloor) using a depth threshold and further used as reef mask layer. The depth threshold is defined as the average depth of all grid cells identified as planes (zonal statistics). To map the outer-reef crest, peaks were used as primary features inside the reef mask layer with at least a "moderate" rugosity. Patches of bioturbation occurring on the seafloor are mainly characterised by pit clusters (primary feature). Planar areas inside the reef mask layer with "very low" rugosity were used as primary features for the reef flat according to Hopley (1982). Upper-reef flat zones are generally exposed at the leeward margin to the northwest and this planar zone becomes interrupted by isolated reef boulders towards this side (Hopley, 1982). To exclude planar areas towards the leeward margin, the depth threshold was again updated to the average depth of all planar features within the reef mask layer. Finally, to join isolated, small or disconnected areas, the morphological closing operator has been applied on the primary morphometric feature class.

2.6. Ground-truthing

Classification results were verified with underwater towed video data. The location of the video data was corrected for the layback offset by recognition of features uniquely identifiable in both video and multibeam data, such as coral isolates or conspicuous bommies (greater than 3 m in size). The potential drift of the camera in a perpendicular direction to the vessel track was not taken into account. The video data were classified by visual inspection of individual video frames in time steps of 5 s, representing approximately 5 m distance at a tow speed of 2 kn. Classes used were bare seafloor (including sparse cover of algae and seagrass), bioturbation and coral reefs. Coral reefs were further subdivided according to their coral coverage into: isolated patches, sparse, medium and dense coral cover, whereby the level of cover was chosen by visual estimation.

3. Results

Biquadratic surface fitting was used to calculate surface parameters (i.e. slope, cross-sectional curvature, rugosity) from the DBM for scales (i.e. kernel sizes) from 5 to 35 m. A subset of the resulting morphometric feature classes is shown in Fig. 5 for 5 to 17 m, in which a trend in the reduction of feature class variety proportional with kernel size is apparent. Kernel sizes of more than 19 m were not suitable for feature identification of structures smaller than 3 m in diameter. The result of an applied 35 m filter kernel is shown in Fig. 10 (centre), in which the majority of features were identified as planes (yellow areas) even where boulders are apparent in sun-illuminated shaded DBM (cf. discussion in Section 4). It is worthwhile mentioning that the result for the 19 m filter kernel in Fig. 5 is not shown, due to

Table 1
Surface-fitting accuracy examined by RMS error calculation for circular kernel shapes.

Kernel size	Min	Max	Standard deviation	Average
5	0.000	0.858	0.007	0.007
7	0.000	0.995	0.014	0.014
9	0.002	0.964	0.020	0.019
11	0.003	0.964	0.028	0.027
13	0.004	1.057	0.035	0.032
15	0.004	1.119	0.041	0.038
17	0.005	1.215	0.049	0.044
19	0.005	1.307	0.057	0.050

All values given in meters providing statistics about minimum, maximum, standard deviation and average.

Please cite this article as: Zieger, S., et al., Mapping reef features from multibeam sonar data using multiscale morphometric analysis, Mar. Geol. (2009), doi:10.1016/j.margeo.2009.06.002

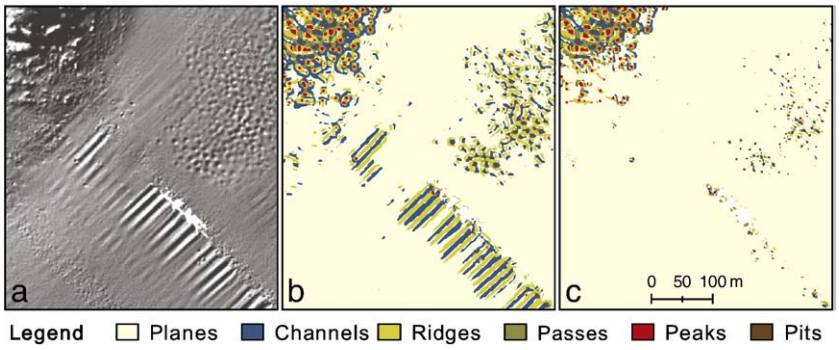

Fig. 6. Apparent motion residuals on the seafloor (a) identified as channels and ridges (b) were replaced by planes outside the reef mask layer where the slope is less than 10° (c).

similarity to the result of the 17 m kernel. Classification parameters were set to 35° for slope (*slopemin*) and 0.012 for minimum cross-sectional curvature (*crocmin*) and remain constant for all scales used.

The performance of the surface fitting is very high and was examined using root mean square (RMS) error calculation (Table 1). The average RMS error (RMSE) of datasets in use is 2.9 cm (for kernel sizes: 5 to 19 m) and less than 0.3% of the kernel size for each scale. With increasing kernel size, the RMSE increases indicating that the largest errors are most prominent at steep slopes (reef edges) and data gaps on seafloor areas besides the platform reef.

On the flat seafloor, morphometric features largely identified DBM related artefacts (Fig. 6a) as channels and ridges (Fig. 6b). To avoid misinterpretation by non-experts, these areas were replaced by planes.

To determine the dominant morphometric feature class over all suitable scales (5 to 19 m), multiscale fuzziness was carried out in which double weights ($\omega = 2.0$) were applied to scales from 9 to 13 m to suppress distinctive misclassified reef features, as demonstrated in Fig. 7. Variations of morphometric feature class over spatial scale were examined by the entropy (Fig. 8). High entropy appears on inner-reef flat areas and in patches besides the platform reef respectively, whereas major reef bommies and bare seafloor are characterised by low entropy.

Ground-truthing provided evidence that on the submerged platform reef, both outer-reef crest and inner-reef flat areas are covered by a medium to dense coral veneer. A distinctive change of coral cover (i.e. from dense to thin coral veneer), between outer-reef crest and inner-reef flat, is not present; however, a dense coral coverage on the outer-reef crest has been clearly identified and visually confirmed by video surveys. On the flat seafloor around the reef, various regions were identified as significantly modified by meter-scale bioturbation by large benthic organisms, which results in depressions of generally circular shape in seafloor sediments. This is a previously undescribed extension of the Hopley classification scheme. Patches of bioturbation are clearly characterised by clusters of holes ranging from 80 to 200 m in size (Fig. 9).

4. Discussion

Terrestrial classification parameters for morphometric features suggested by Wood (1996) and Fisher et al. (2004) (i.e. for highlands *slope* 1° and 4°) are not applicable and would tend to focus on planes, channels, and ridges as the dominant morphometric features, while underestimating peaks and pits. Due to the biogenic origin of features and the very high relief terrain, slope-threshold was increased to 35°. As described by Hopley (1982), coral reefs feature near-vertical barriers and steep slopes, similar to tabletop mountains in terrestrial landforms which are difficult to model using spatial analysis.

Adjusting the kernel size was carried out here, but when increasing the size of the filter kernel, seafloor features were classified more often as channels and ridges rather than peaks and pits, while circular shapes were still identified correctly (Fig. 10). In Fig. 10, results appear similar for a scale of 17 and "virtual" 34 m (17×17 kernel applied to 2 m cell size DBM) using constant parameters within decision tree classifier. Note that a test on a resampled DBM (2 m cell size) led to different morphometric features by labelling peaks in the form of a ring instead of a circular disc (e.g. for coral boulders).

Inner-reef flat and bioturbated areas show a high variety of morphometric features when altering spatial scale. These zones are characterised by planar areas on small scales, and are composed of pinnacles, holes, passes, ridges and channels on larger scales. The inner-reef flat in particular shows the highest average entropy (Table 2).

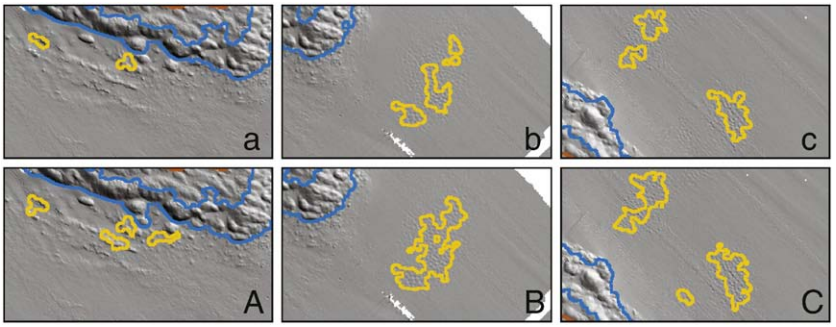

Fig. 7. Enhancement of reef feature extraction method for patches of bioturbation (yellow zones) by applying different weight factors to different scales in contrast to an equal weight approach (a,b,c). In subfigures A,B,C double weights were used for scales ranging from 9 to 13 m.

Please cite this article as: Zieger, S., et al., Mapping reef features from multibeam sonar data using multiscale morphometric analysis, Mar. Geol. (2009), doi:10.1016/j.margeo.2009.06.002

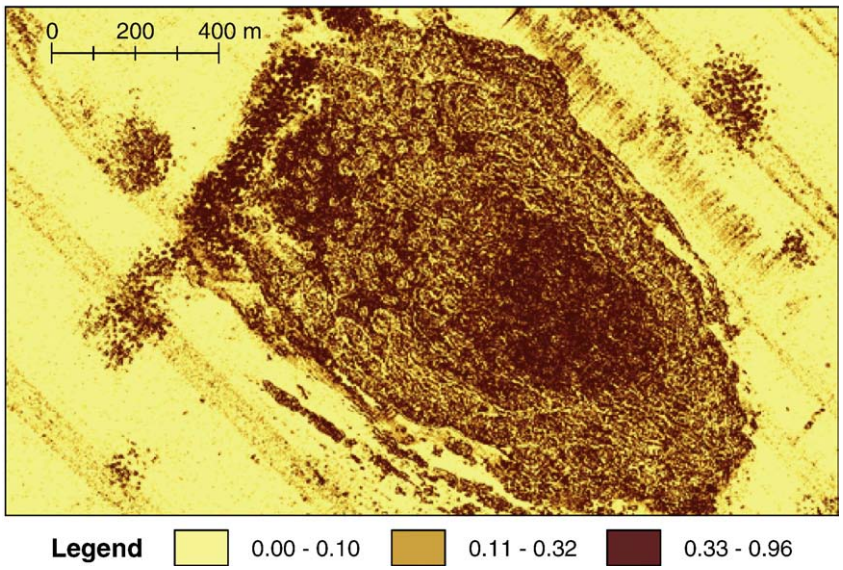

Fig. 8. Entropy measurements E_x based on Eq. (7) showing morphometric class variation. Values range between zero (no variation at all) and one (classification split equally at all scales).

The presented feature extraction method mainly uses peaks, pits and planes in combination with depth to identify classes and Table 2 summarises the distribution of feature classes of each mapped reef zones. Hopley (1982) also described "spur-and-grove" systems, aligned to the major wave direction and frequently present on high-energy outer-reef edges and reef fronts. Ground-truthing revealed the importance of these forms in providing shelter and breeding grounds for creatures of the coral reef community. We suggest that such channels may be considered an additional habitat class. While the outer margin of the rim is well defined and identified correctly, inner boundaries are less well defined as a result of the continuous nature of the reef morphology of both inner-reef flat and outer-reef crest. Modern sea-level reefs with sandy, slightly depressed inner-reef flat areas may allow more precise boundary identification.

Weight factors can be used to map some zones more precisely, but the misclassification rate slightly increases at locations composed of similar responding morphometric features (i.e. isolated off-reef coral boulders) that will produce pits when they occur in dense formations (cf. Fig. 7A). As shown in Fig. 7a, the method is not designed to separate between real pits and the flat seafloor encircled by off-reef coral boulders. Indeed, adjusting the depth threshold will eliminate misclassified areas; but note, however, that it will also remove valuable areas like zones inside lee-side sediment layers.

An attempt was made to apply the morphometric analysis to data affected by motion artefacts, which are present in many surveys that are not carried out to dedicated survey standards. The primary motivation for the inclusion of these data was the compromised data

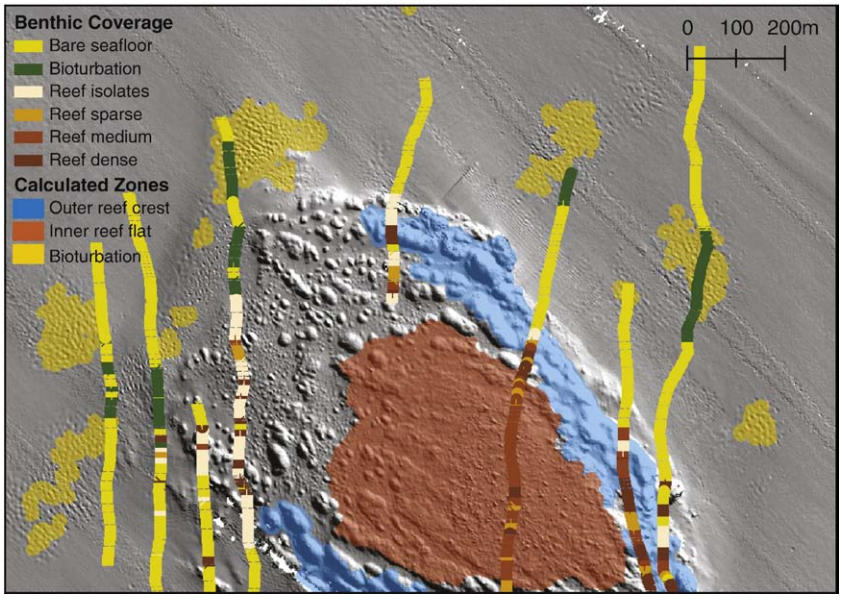

Fig. 9. Ground-truthing results showing a sun-illuminated DBM in the background, overlaid by mapped reef features and layback corrected transect surveys.

Please cite this article as: Zieger, S., et al., Mapping reef features from multibeam sonar data using multiscale morphometric analysis, Mar. Geol. (2009), doi:10.1016/j.margeo.2009.06.002

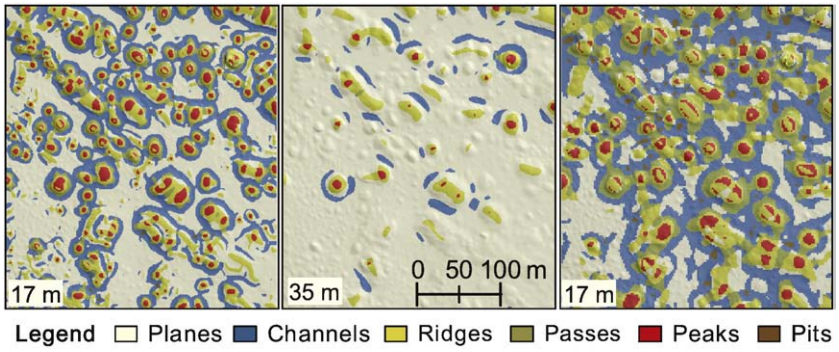

Fig. 10. Sensitivity of kernel sizes within the morphometric feature extraction method for 1 m (left and centre) and resampled 2 m (right) DBMs. Comparing left and right subfigures, the approach appears to be more sensitive to kernel size rather than the real numeric scale (resolution). Features were extracted using constant thresholds of: *slope* = 35° and *crosc* = 0.012.

coverage if this erroneous data had been removed; in other words, the erroneous data still contained some valuable information (e.g. it was still possible to assess the presence or absence of bioturbation etc).

Reassigning motion residuals (artefacts) from channels and ridges to planar features needed to be carried out to avoid misclassification. However, with this step, valuable morphometric information was also removed from the seafloor (i.e. within bioturbated areas). Table 2 shows a clear reduction of channels and ridges for bioturbation. It is not trivial to remove artefacts from the bathymetric model directly to preserve morphometric information, because they appear condensed in various swaths where the rate of error rapidly increases in cross-track direction. However, a surface model (DBM) with a small number of artefacts could lead in more precise habitat classification when including channels and ridges to the identification method, particularly for habitats on the seafloor. Here, results have shown that artefacts are similar in size and trend and may be removed with alternative methods e.g. with principal component analysis.

5. Conclusion

High-resolution multibeam sonar data were classified by analysing the small-scale seafloor geomorphology. A surface-approximation approach combined with multiscale fuzziness modified from terrestrial land analysis was applied to systematically discriminate feature classes on a submerged reef. The classification approach may further be improved by adding morphometric feature variety (entropy) into the classification scheme. The spatial scale of the morphometric surface analysis is a critical parameter in the delineation of classes.

Embedding this method into ArcGIS using Python provides capabilities for a “start to finish” process producing sophisticated reef maps that can assist marine scientists to describe and monitor reef sites systematically, and to collect information about habitat changes as well as biologic activities such as bioturbation.

Table 2
Summary of reef zones with relative morphometric feature distribution (in percent) and average entropy E_x.

	Outer-reef crest	Inner-reef flat	Bioturbation
Planes	10.44	43.94	74.10
Channels	27.18	24.80	5.28
Ridges	27.21	18.18	6.63
Passes	20.80	7.75	7.99
Peaks	11.50	4.08	1.81
Pits	2.88	1.25	4.19
E_x (±stdv.)	0.296 (±0.195)	0.385 (±0.178)	0.248 (±0.187)

Acknowledgements

The work presented here was submitted as a thesis to the Faculty of Forest, Geo and Hydro Sciences at the Dresden University of Technology, Germany (Zieger, 2007). The multibeam data were collected on the AIMS research vessel *RV Lady Basten* in July 2003; tow video data was collected by Peter Speare (AIMS) on the same cruise and subsequently analysed by the authors. We thank John Hughes Clarke (University of New Brunswick, Canada) for providing the multibeam processing software package SwathEd to TS, and Jonathan Beaudoin for SwathEd training. The data collection was funded by the Australian Institute of Marine Science and James Cook University. We also thank Professor Manfred Buchroithner (Dresden University of Technology, Germany) for his constructive comments and support. Four anonymous reviewers greatly improved the manuscript.

References

Bourke, P., 1989. An algorithm for interpolating irregularly-spaced data with applications in terrain modelling. Pan Pacific Computer Conference, Beijing, China.
Buja, K., 2006. The habitat digitizer extension: an ArcGIS 9 extension for delineating and classifying features in georeferenced imagery. Center for Coastal Monitoring and Assessment (CCMA), NOOA's National Centers for Coastal Ocean Sciences. Silver Spring, MD.
Buttler, H., 2005. A guide to the Python Universe for ESRI users. ArcUser Mag. April–June, pp. 34–37. available online at http://www.esri.com/news/arcuser/.
Cartwright, D., Hughes Clarke, J.E., 2002. Multibeam surveys of the Fraser River Delta, coping with an extreme refraction environment. Proc. of the Canadian Hydrographic Conf. Canadian Hydrographic Association, Ottawa, ON.
Dartnell, P., 2000. Applying remote sensing techniques to map seafloor geology/habitat relationships. Master's thesis, San Francisco State University, CA.
Davies, P.J., Cucuzza, J., Marshall, J.F., 1983. Lithofacies variations on the continental shelf east of Townsville: Great Barrier Reef. In: Baker, J.T., M., C. R., P.W., Sammarco, Stark, K.P. (Eds.), Proc. Great Barrier Reef Conf.
Davies, P.J., Marshall, J.F., Searle, D.E., 1981. Shallow inter-reef structure of the Capricorn Group, Southern Great Barrier Reef. J Aust. Geol. Geophys. 6, 101–105.
Evans, I.S., 1980. An integrated system of terrain analysis and slope mapping. Zeitschr. Geomorph. 36, 274–295.
Fisher, P., Wood, J., Cheng, 2004. Where is Helvellyn? Fuzziness of multi-scale landscape morphometry. Trans. Inst. Br. Geogr. 29 (1), 106–128.
Fisher, P.F., 2000. Fuzzy modelling. In: Openshaw, S., Abrahart, R.J. (Eds.), Geocomputing. Taylor and Francis, London, UK, p. 413. Ch. 7.
González, J.E., Done, T.J., Page, C.A., Cheal, A.J., Kininmonth, S., Garza-Pérez, J.R., 2006. Towards a reefscape ecology: relating biomass and tropic structure of fish assemblages to habitat at Davies Reef. Australia. Mar. Ecol. Progr. 320, 29–41.
Greene, H.G., Kvitek, R., Bizzaro, J.J., Bretz, C., Iampietro, P.J., 2004. Fisheries habitat characterization of the California continental margin. California Sea Grant College Program, University of California, CA.
Hopley, D., 1982. The Geomorphology of the Great Barrier Reef: Quaternary Development of Coral Reefs. John Wiley & Sons, Inc, New York.
Hopley, D., Smithers, S.G., Parnell, K.E. (Eds.), 2007. The Geomorphology of the Great Barrier Reef: Development, Diversity, and Change. Cambridge University Press.
Hughes Clarke, J.E., Godin, A., 1993. Investigation of the roll and heave errors present in Frederick G. Creed – EM1000 Data When Using a TSS-335B Motion Sensor. Tech.

Please cite this article as: Zieger, S., et al., Mapping reef features from multibeam sonar data using multiscale morphometric analysis, Mar. Geol. (2009), doi:10.1016/j.margeo.2009.06.002

rep., Department of Fisheries and Oceans, Canada, Contract Report No. FP7007-3-5731.
Iampietro, P.J., Kvitek, R.G., Morris, E., 2005. Recent advances in automated genus-specific marine habitat mapping enabled by high-resolution multibeam bathymetry. Mar. Tech. Soc. J. 29 (3), 83–93.
Jenness, J.S., 2002. Calculating landscape surface area from digital elevation models. Wildl. Soc. Bull. 32 (3), 829–839.
Johnson, D.P., Searle, D.E., Hopley, D., 1982. Positive relief over buried post-glacial channels, Great Barrier Reef Province, Australia. Mar. Geol. 46 (1), 149–159.
Jordan, A., Davies, P., Ingleton, T., Pritchard, T., 2006. Application of swath acoustic technology as a tool for seabed habitat mapping in coastal waters of New South Wales, Australia. Proc. of CoastGIS 2006 – GIS for the Coastal Zone: Spatial Data, Modelling and Management, vol. 16. Woolongong Papers on Maritime Policy, University of Woolongong, Australia.
Jupp, D.L.B., Mayo, K.K., Kuchler, D.A., Claasen, D.V.R., Kenchington, R.A., Guerin, P.R., 1985. Remote sensing for planning and managing the Great Barrier Reef of Australia. Photogrammetria 40 (1), 21–42.
Lanier, A., Romsos, C., Goldfinger, C., 2007. Seafloor habitat mapping on the Oregon continental margin: a spatially nested GIS approach to mapping scale, mapping methods, and accuracy quantification. Mar. Geodes. 30 (1), 51–76.
Lucieer, V., Pederson, H., 2008. Linking morphometric characterisation of rocky reef with fine scale lobster movement. ISPRS J. Photogram. Rem. Sen. 63, 496–509.
Lundblad, E.R., Wright, D.J., Miller, J., Larkin, E.M., Rinehart, R., Naar, D.F., Donahue, B.T., Anderson, S.M., Battista, T., 2006. A benthic terrain classification scheme for American Samoa. Mar. Geodes. 29 (2), 89–111.
Mitchell, N.C., Hughes Clarke, J.E., 1994. Classification of seafloor geology using multibeam sonar data from the Scotian Shelf. Mar. Geol. 121, 143–160.
Orme, G.R., Flood, P.G., Sargent, G.E.G., 1978. Sedimentation trends in the lee of outer (ribbon) reefs, Northern region of the Great Barrier Reef province. Phil. Trans. Roy. Soc. Lond. 291, 85–99.
Orme, G.R., Salama, M.S., 1988. Form and seismic stratigraphy of Halimeda banks in part of the northern Great Barrier Reef Province. Coral Reefs 6 (3–4), 131–134.
Pitcher, C.R., Doherty, P., Arnold, P., Hooper, J., Gribble, N., Bartlett, C., Browne, M., Campbell, N., Cannard, T., Cappo, M., Carini, G., Chalmers, S., Cheers, S., Chetwynd, D., Colefax, A., Coles, R., Cook, S., Davie, P., De'ath, G., Devereux, D., Done, B., Donovan, T., Ehrke, B., Ellis, N., Ericson, G., Fellegara, I., Forcey, K., Furey, M., Gledhill, D., Good, N., Gordon, S., Haywood, M., Hendriks, P., Jacobsen, I., Johnson, J., Jones, M., Kinninmoth, S., Kistle, S., Last, P., Leite, A., Marks, S., McLeod, I., Oczkowicz, S., Robinson, M., Rose, C., Seabright, D., Sheils, J., Sherlock, M., Skelton, P., Smith, D., Smith, G., Speare, P., Stowar, M., Strickland, C., Van der Geest, C., Venables, W., Walsh, C., Wassenberg, T., Welna, A., Yearsley, G., 2007. Seabed biodiversity on the continental shelf of the Great Barrier Reef World Heritage Area. AIMS/CSIRO/QM/QDPI CRC Reef Research Task Final Report, 320 pp.
Richards, K.S., 1981. Introduction to morphometry. In: Goudie, A.S. (Ed.), Geomorphological Techniques. Allen and Unwin, London, pp. 25–30.
Robinson, V.B., 1988. Some implications of fuzzy set theory applied to geographic databases. Comput. Environ. Urban. Syst. 12, 89–97.
Sierra, J., 1982. Image Analysis and Mathematical Morphology. Academic Press, London, England.
Weiss, A., 2001. Topographic position and landforms analysis. Poster presentation, ESRI User Conf., San Diego, CA.
Wilson, M.F.J., O'Connell, B., Brown, C., Guinan, J.C., Grehan, A.J., 2007. Multiscale terrain analysis of multibeam bathymetry data for habitat mapping on the continental slope. Mar. Geodes. 30 (1), 3–35.
Wood, J. D., 1996. The geomorphological characterisation of digital elevation models. Ph.D. thesis, University of Leicester, UK.
Zieger, S., 2007. Biotic classification of multibeam sonar data of a coral reef in the Great Barrier Reef, Australia. Master's thesis, Dresden University of Technology, Institute for Cartography, Germany.

Please cite this article as: Zieger, S., et al., Mapping reef features from multibeam sonar data using multiscale morphometric analysis, Mar. Geol. (2009), doi:10.1016/j.margeo.2009.06.002